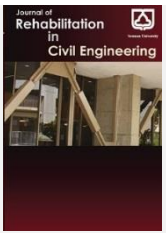

Journal of Rehabilitation in Civil Engineering

Journal homepage: https://civiljournal.semnan.ac.ir/

An Experimental Study on the Effect of Using Embedded Glass Fiber Geogrid Mesh on the Flexural Behavior of Concrete Beams

Mohammad Dashtpour [1]; Seyed Shaker Hashemi [2,*]; Mahmoud Malakouti Oloun Abadi [3]

1. Department of Civil Engineering, Persian Gulf University, Shahid Mahini Street, Bushehr, P.O. Box 75169-13817, Iran
* Corresponding author: *sh.hashemi@pgu.ac.ir*

ARTICLE INFO

Article history:
Received: 05 January 2024
Revised: 16 May 2024
Accepted: 01 August 2024

Keywords:
Glass fiber geogrid mesh;
Flexural strength;
Reinforced concrete beams;
Geogrid mesh layers.

ABSTRACT

Nowadays, concrete is one of the most commonly used building and pavement materials. The type of concrete that has been used more than the other types is the concrete reinforced with steel. Due to the disadvantages of reinforcing concrete with steel such as corrosion, heavy weight, high cost and high-energy production, Glass Fiber Geogrid Mesh (GFGM) is chosen in this study for investigating the flexural reinforcement in the concrete beams. Fifty concrete beams in dimensions of 65 cm × 15 cm × 15 cm with different layers of GFGM, placements, curing times (28 and 90 days) and various concrete mixing designs (25 and 30 MPa) were reinforced in order to be compared with the unreinforced concrete beams (control beams). Then, the beams were tested under three-point bending test using displacement control mechanism. The results showed that the peak load capacity increased at most to 48.6 % in comparison with the Control Beams. Furthermore, a complete bonding between the GFGM and the concrete was indicated. It was also observed that the deflection at the midspan of the specimens reinforced with different Geogrid placements did not follow a specific pattern.

E-ISSN: 2345-4423

How to cite this article:
Dashtpour, M., Hashemi, S. S., & Malakouti Oloun Abadi, M. (2025). An Experimental Study on the Effect of Using Embedded Glass Fiber Geogrid Mesh on the Flexural Behavior of Concrete Beams. Journal of Rehabilitation in Civil Engineering, 13(2), 171-186.
https://doi.org/10.22075/jrce.2024.32888.1970

1. Introduction

Concrete is one of the most commonly used building materials, a brittle material with a tensile strength of about one tenth of its compressive strength. For this reason, concrete products are often reinforced with steel. Nowadays, the advancement of science and technology, indicates that paying attention to resistance as a criterion for the concrete design cannot solve the problems that occur in the long-term in the concrete structures. In this regard, the durability of concrete in different environments has been recently considered as a problem in the design of the concrete structures [1–4]. Furthermore, observing physical and chemical breakdowns of concrete in most parts of the world, especially in the developing countries has pushed thoughts and minds toward designing a concrete with more specific and durable features. One of the new materials which has gained a special place in the construction industry is the reinforcing fibers.

The fibers exist in two different forms, either continuous or discrete, which have been used extensively in different parts of the building. In terms of type, the reinforcement fibers have been divided into three categories: natural (flax, coir, jute etc.), synthetic (polyester, polypropylene, carbon, PBO, aramid) [5] and metal (generally steel) [6]. In terms of shape, the reinforcement fibers can be either short dispersed fibers or continuous fibers that are mostly in the form of a mesh or fabric, referred to as textile [7–9]. More specifically, the continuous fibers exist in various shapes and designs, which can be used in different ways for the reinforcement purposes [10–12].

One of the applications of the continuous fiber is to rehabilitate the structures. Since the 1990s, the combination of fiberglass mesh embedded in epoxy matrix, the so-called civil engineering FRP (Fiber Reinforced Polymer) has been successfully used for repairing and strengthening the flexural and shear capacities of the reinforced concrete members of various structures including beams, columns and slabs [7,13,14]. Another application of the continuous fiber is the use of cement-based composite systems. These cement-based composites were later called FRCM (Fiber Reinforced Cementitious Matrix) [15,16]. The FRCM consists of the continuous fiber in the form of a net or fabric mesh embedded in a cementitious matrix and used as an external reinforcement [17–20].

One example of the continuous fiber is a geogrid mesh that is divided into four categories of Plastic Geogrid, Fiber Glass Geogrid, Steel Geogrid and Polyester warp-weft Geogrid. The Glass Fiber Geogrid Mesh (GFGM) is made of glass fiber and the roving as the main raw material. This product is composed of glass fiber filaments that are coated with an inorganic agent. Some advantages of the GFGM are its high tensile strength in warp across directions, low elongation, high flexibility, high and low temperature resistance, physical and chemical stability. Some applications of this product are reinforcing the asphalt and concrete pavements, reinforcing soil substrates and preventing cracks that occur due to shrinkage [21,22].

A few studies have been conducted to evaluate the use of geogrid mesh in concrete members. Meng et al. [23] investigated the flexural behavior of the concrete beams reinforced with the polypropylene biaxial geogrid. The effects of the embedded geogrid mesh on the porosity level, the cracking behaviors and strength were investigated in their study. They found that, due to using the embedded geogrid mesh, despite the increased porosity, a significant post-crack performance was indicated. In another study, Tang et al. [24] investigated the flexural behavior of the concrete beams reinforced with triaxial polypropylene Geogrid under a four-point bending test. In their study, the results showed that embedding the geogrid improved the ductility of the post-peak behavior of the concrete beam and delayed the rupture failure of the concrete beam. In their study, no slippage was observed between the geogrid and the concrete. Moreover, Tang et al. [25] investigated the behavior of Geogrid -reinforced Portland Cement Concrete (PCC) beams. They indicated that reinforcing the

beams with the geogrid led to a significant ductility after crack initiation in the concrete and different failure modes were observed for PCC beams. They also found that the flexural strength of the concrete-reinforced beams was not necessarily improved due to the inclusion of the geogrid. Al-Hedad et al. [26] investigated the effect of geogrid reinforcement on the drying shrinkage of High-Strength Concrete (HSC) pavements. They found that the geogrid led to the reduction of the drying shrinkage strains of HSC.

Many studies have investigated the use of fiber products for reinforcing the concrete members. For example, Erfan et al. [27] studied the flexural behavior of Nano Concrete (NC) and HSC beams reinforced with GFRP bar. They found that the nano-concrete mix had no effect on increasing the concrete strength, but improved the behavior of beam's cracks in bending while decreasing its number and width. In a similar study, Ahmed et al. [28] investigated the flexural strength and failure of the geopolymer concrete beams reinforced with carbon fiber-reinforced polymer (CFRP) bars. The results showed that the deflection decreased and the first cracking load increased by increasing the compressive strength. Moreover, in the geopolymer concrete beams, the crack width was lower value than the ordinary Portland concrete beams.

Due to the disadvantages of reinforcing concrete with steel such as corrosion, heavy weight, high cost and high-energy production and also due to the advancement of science in the construction industry and production of new building materials, the use of continuous fibers can be considered as a good method for reinforcing the concrete. In the same regard, since there have been no comprehensive studies on the use of GFGM for reinforcing concrete members, the current study attempts to reinforce the flexural strength of the concrete beams with GFGM in different layers and positions as an alternative to steel reinforcement, and to evaluate the performance of this production.

2. Material properties

The experimental program includes two main parts. The first part consists of the mechanical properties of the GFGM as well as the characteristics of the concrete used. The second part includes preparing and testing the concrete beams.

2.1. Characterization of the GFGM

In the current study, GFGM is used for reinforcing the concrete beams. It is worth mentioning that the GFGM used in this study were of the kN50x50 type, with openings of 25 millimeters and a tensile strength of 50 kilo-Newton per meter. The weight of these GFGM per one layer was 230 grams per square meter (Fig. 1).

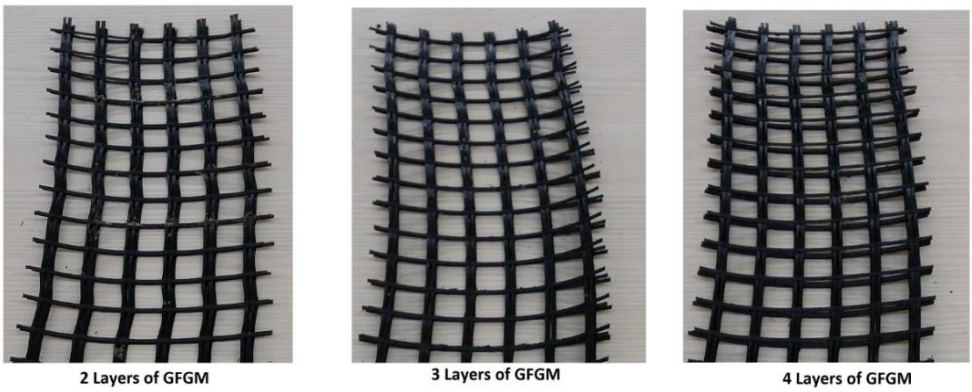

Fig. 1. A few samples of the embedded GFGM used in the concrete beams.

2.2. Characteristics of the concrete

To prepare the specifications of the materials used in concrete, three experimental groups have been performed.

- Aggregates experiments
- Concrete experiments
- Fresh concrete experiments

Approximately 70 to 80 percent of the concrete volume is made of aggregates. Thus, they play an important role in the properties and performance of concrete. Therefore, experiments of sieve analysis of fine and coarse aggregates and fineness module were performed according to ASTM C136 [29], bulk density (unit weight) and voids in aggregate experiment was performed according to ASTM C29 [30], total evaporable moisture content of aggregate experiment was performed according to ASTM C566 [31] and the experiment of density, relative density (specific gravity), and absorption of coarse and fine aggregate was performed according to ASTM C127 [32] and C128 [33]. In this regard, the grading of aggregates was performed based on the limits provided by ASTM C33 [34] and the coarse aggregate with a maximum size used in the preparation of concrete is 19 mm.

The cement used in the current study was of Portland type II. To determine the specifications of the used cement, the density hydraulic cement experiment was performed according to ASTM C188 [35], the experiment of time of setting of hydraulic cement was performed according to ASTM C191 [36], compressive strength of hydraulic cement experiment was performed according to ASTM C109 [37] and in order to determine the rest of its specifications, the certificate provided by the manufacturer was used.

It should be noted that the concrete mixing design used in this study was designed based on ACI 211 concrete mixing design [38]. In this study, in order to prepare the beams, two concrete mixing designs with 28-day nominal compressive strength of 25 MPa and 30 MPa were used. The water/cement ratio was 0.491 and 0.435 for the concrete mixing designs of 25 MPa and 30 MPa, respectively. The slump value of 8 cm was indicated by the concrete prepared for both mixing designs according to ASTM C143 [39]. In addition, the density unit weight of 2336 and 2344 kilograms per cubic meter were indicated for the mixing design of 25 and 30 MPa, respectively (ASTM C138 [40]). Details of the mixing designs are shown in the Table 1.

Table 1. Mixture proportion of the concrete (kg per cubic meter).

Mixture Material / Concrete Type	Cement	Water	Coarse Aggregate	Fine Aggregate
Concrete 25MPa	417.51	205	778.3	968.71
Concrete 30MPa	471.26	205	778.3	921.02

In order to evaluate the concrete mixing designs (25 and 30 MPa), six cylindrical specimens with a diameter of 15 cm and a height of 30 cm were prepared from both concrete mixing designs. The specimens were then kept in the controlled temperature and the humidity conditions for 28 days to be tested for the compression. After 28 curing days, the specimens made for both mixing designs indicated an average compressive strength of 25.4 MPa and 30.02 MPa, respectively (ASTM C39 [41]).

3. Laboratory planning

3.1. Preparation of specimens

The specimens used in this study are concrete beams in dimensions of 65 cm ×15 cm ×15 cm, which are reinforced with GFGM in various scenarios.

The most important parameters studied in this research are:

Layers of GFGM

Concrete mixing design

The placement of the GFGM in the cross-section beam

Curing time (28 days and 90 days)

For reinforcement of the concrete beams, the GFGM is embedded in different layers (varies from 1 to 5) at different distances (10 mm, 20 mm, 30 mm) from the tensile face of the concrete beams. Increasing the number of layers increases the density of the GFGM inside the specimen. The specimens are named as $B_iL_jR_kD_m$, where the letter″ B″ refers to the type of the specimen (Beam) and its index (i) refers to the standard cylindrical compressive strength (in MPa) of the used concrete at 28 days. The letter″L″ with its index (j) refer to the number of layers of GFGM used in the specimen. For each reinforced beam model, all of the Geogrid layers are placed together (on each other) and located in the beam section according to the R ratio. The letter″ R″ with its index (k) refer to the relative placement of the GFGM (k=H/X), which H indicates the height of the beam section (15 cm) and X indicates the distance between the placement of the GFGM and the bottom face of the section (As shown in Fig. 2). The letter″D″ with its index (m) refer to the curing time of the specimens (28 days and 90 days). For example, in the $B_{25}L_3R_{15}D_{28}$ model, the compressive strength of the concrete is 25 MPa and three layers of GFGM are placed at a distance of 1 cm from the lower face of the beam and the specimen was tested at the age of 28 days.

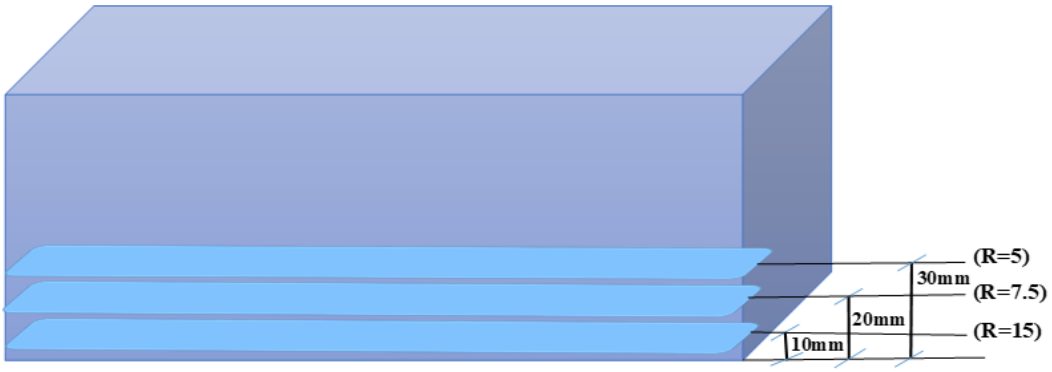

Fig. 2. Different placements of GFGM at the tensile face of concrete beams.

First, the metal molds were lubricated and then the concrete was prepared according to the above-mentioned concrete mixing design. One layer of concrete was cast on the mold and then the GFGM were embedded in the concrete. Second, a more concrete layer was cast on the GFGM and then the specimens were compacted using a vibration table, as shown Fig. 3. In the next stage, the specimens were cured for 24 hours in the mold according to ACI 308-R-01 [42], recommendations for concrete curing and then demolded. Next, the concrete beams were cured in water at 23±1°C for 28 and 90 days, and then tested.

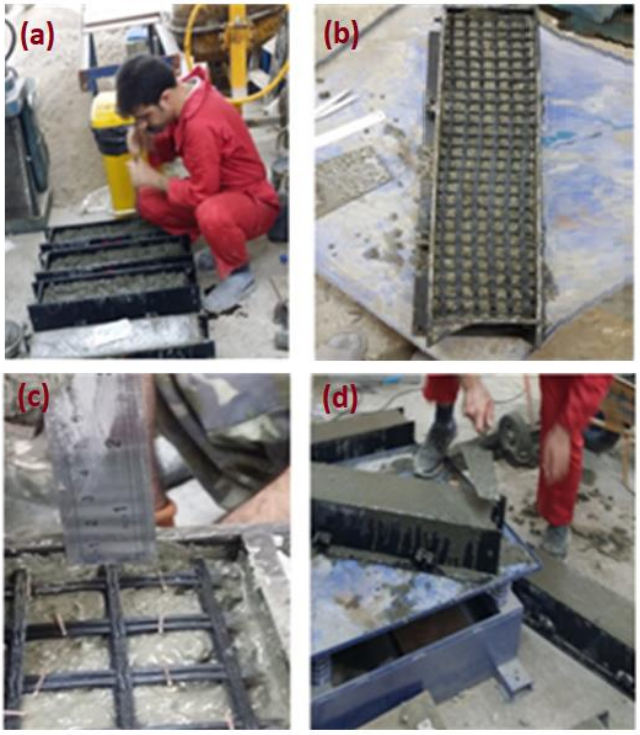

Fig. 3. (a) Casting the first part of fresh concrete; (b) Placing the GFGM; (c) Controlling the placement of GFGM (d) Casting the second part of the concrete and compacting the specimen by the vibration table.

Six unreinforced beams (without GFGM) were prepared for both concrete mixing designs as the Control Beams in order to make a comparison with the reinforced beams during the experiment. It should be considered that for R=15, only 28-day concrete beams were produced.3.2. Test set-up and instrumentations.

After 28 and 90 curing days, the concrete beams were tested in terms of the flexural strength using a three-point bending digital jack machine according to ASTM C293 [43]. This machine consists of one jaw at the upper load and two jaws at the bottom as the fixed supports with a span of 500 mm. A three-point bending test set-up and a schematic of the flexural test setup is indicated in (Fig. 4. and Fig. 5.), respectively.

Fig. 4. Three-point bending jack machine used in the research.

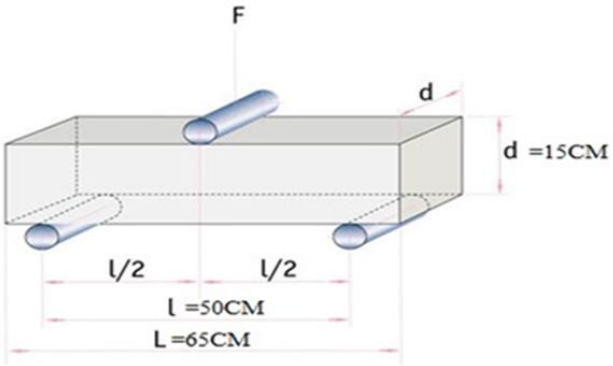

Fig. 5. Schematic and specimen dimensions in the flexural test setup.

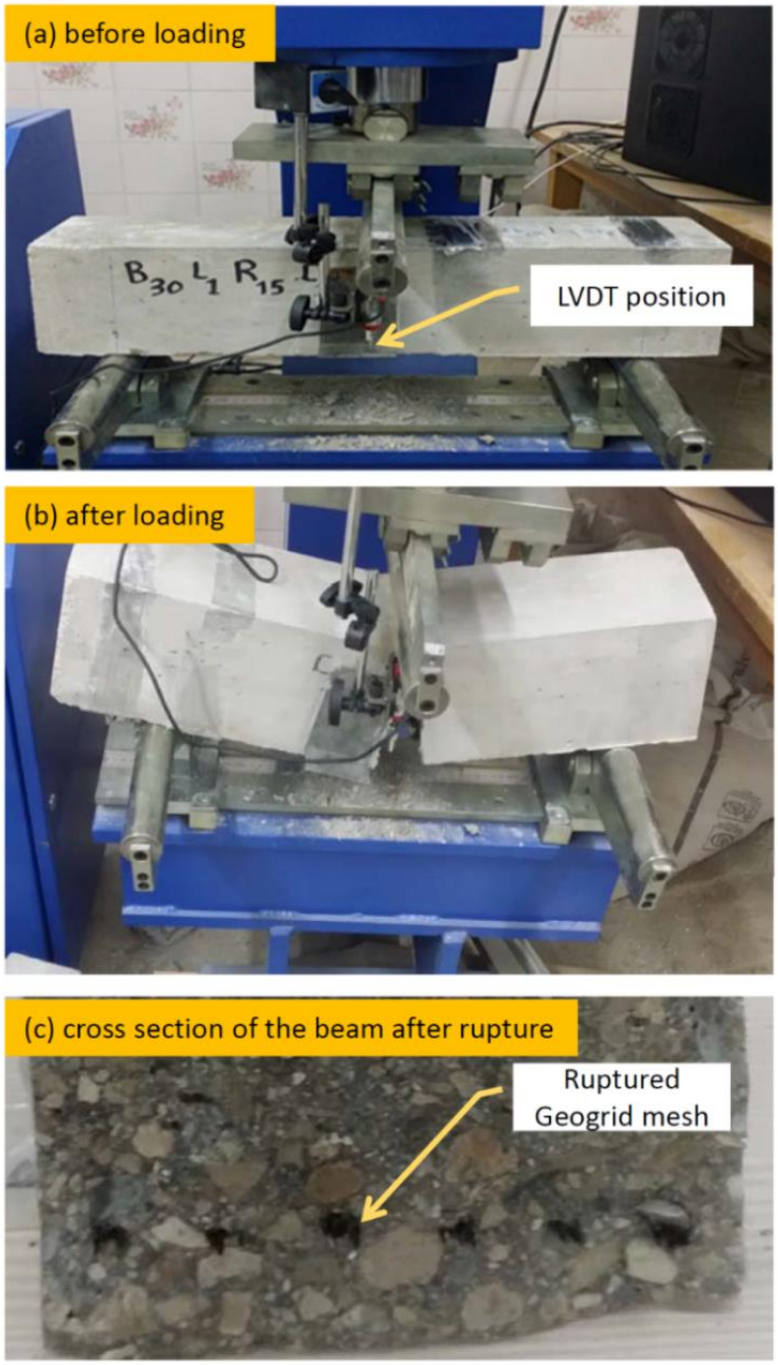

Fig. 6. A detailed sample of the tested specimen and its cross-section. 4. Results and discussion.

As indicated, the beams are placed on the machine in a way that the GFGM is under the tensile load. The Linear Variable Differential Transformer (LVDT) recorded the mid-span displacement of the laboratory specimens during the test as shown in Fig. 6. The LVDT exhibits an accuracy of 0.001 mm, operating under a displacement-control test. The test was conducted at a controlled speed of 0.001 mm per second, ensuring that all tests were subjected to the same loading rate.

The main findings of this study are summarized and evaluated in three sub-sections. According to the ASTM C293 [43], the flexural behavior of concrete is reported in the form of rupture modulus, which indirectly evaluates the tensile strength of concrete. Since the rupture modulus is calculated directly based on the amount of force borne by the beam, therefore, the comparative evaluation of the amount of load carried by the beam is directly related to the evaluation of the flexural behavior of that. From this point of view, in this section, instead of calculating the rupture modulus and expressing it, the amount of load carried by the beam and the force- displacement relationship in the mid-span of the beam have been investigated.

4.2. Investigation of the peak load capacity

4.1.1. Investigation of the peak load capacity for R=5 specimens

Table 2 shows the peak load capacity of the reinforced specimens with the ratio of R=5. In this regard, it was found that increasing the layers of the GFGM from L=1 to L=5 indicated no significant increasing effect on the peak load capacity in comparison with the control concrete beam. In this regard, the highest increase amount was observed for the $B_{25}L_5R_5D_{28}$ specimen with a 19.8% increase in the peak load capacity compared to the Control beam.

Table 2. Results of the peak load capacity for R=5 specimens.

Specimen ID	B25		B30	
	Peak Load (Kg)	Relative Difference Compared to Control Beam (%)	Peak Load (Kg)	Relative Difference Compared to Control Beam (%)
Control Beam	1928.4	—	2062.9	—
$L_1R_5D_{28}$	2038.0	5.7	2106.7	2.1
$L_2R_5D_{28}$	2095.3	8.7	2155.7	4.5
$L_3R_5D_{28}$	2174.3	12.8	2256.4	9.4
$L_4R_5D_{28}$	2148.3	11.4	2265.4	9.8
$L_5R_5D_{28}$	2309.7	19.8	2335.8	13.2

As shown in the Table 2, with increasing the layers of GFGM from $B_{25}L_3R_5D_{28}$ to $B_{25}L_4R_5D_{28}$, the peak load capacity decreased slightly. The reason of this decrease can be due to the defective failure of the $B_{25}L_4R_5D_{28}$ specimen. Fig. 7. shows the load- displacement relationship of the concrete beams reinforced with R=5.

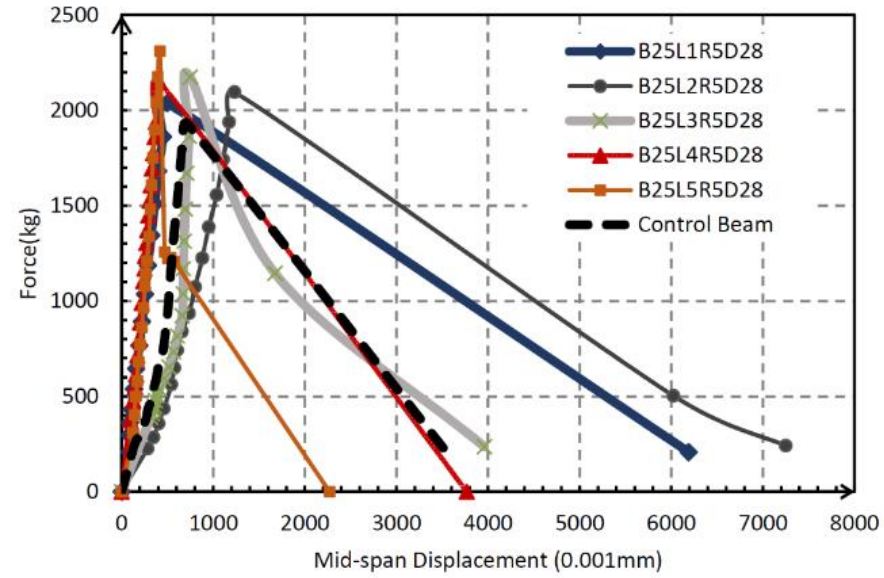

(a): B25 Specimens

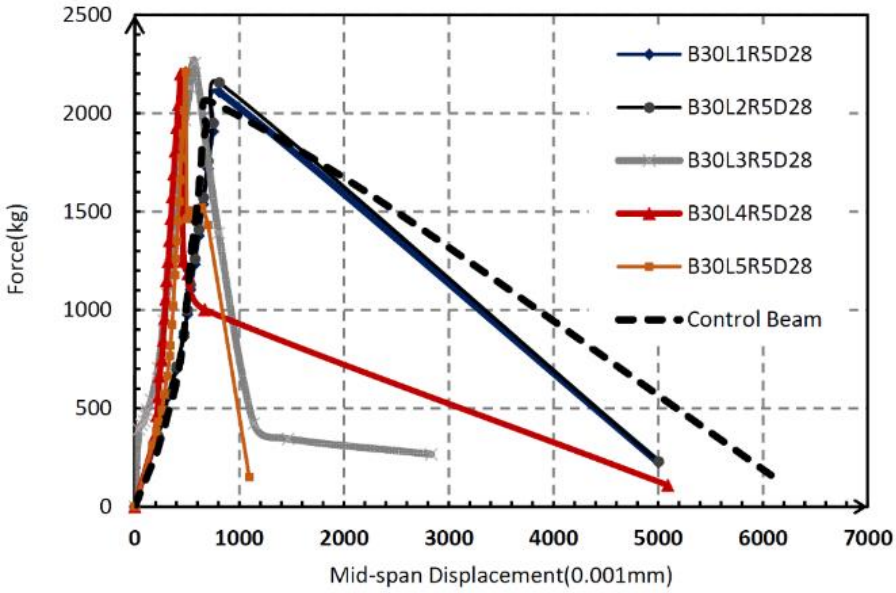

(b): B30 Specimens

Fig. 7. Load- displacement curves at the mid-span for the specimens with R=5.

4.1.2. Investigation of the peak load capacity for R=7.5 specimens

Table 3 shows the peak load capacity of the reinforced specimens with the ratio of R=7.5. In the specimens with the ratio of R=7.5, the reinforcement of the specimens with GFGM indicated a higher impact on the peak load capacity of the specimens in comparison with the Control Beam. It was also found that reinforcing the concrete beams with 1layer GFGM in proportion to 5 layers increased the peak load capacity to 20.5 % and 34.9 % compared to the Control beam, respectively.

Regarding the effect of layers, it was found that increasing the layers of GFGM to 5 indicated no significant effect on the peak load capacity compared to the one-layer reinforced GFGM. Furthermore, it was observed that the $B_{30}L_5R_{7.5}D_{28}$ specimen indicated the maximum peak load capacity with a 16.4% increase value compared to the $B_{30}L_1R_{7.5}D_{28}$ specimen. Fig. 8. Shows the load-displacement relationship of the concrete beams reinforced with R=7.5.

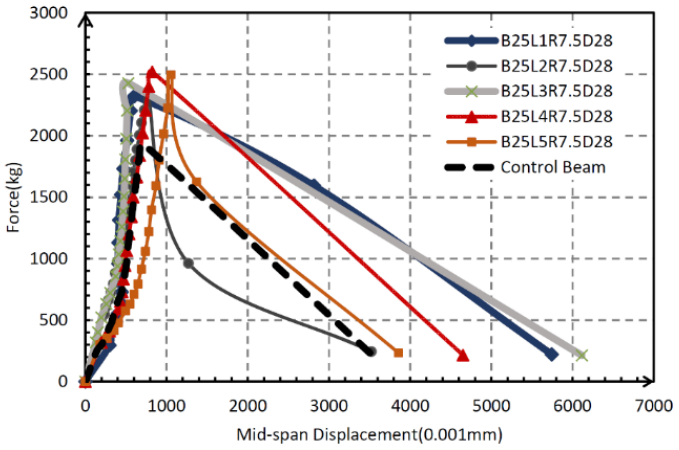

(a): B25 Specimens

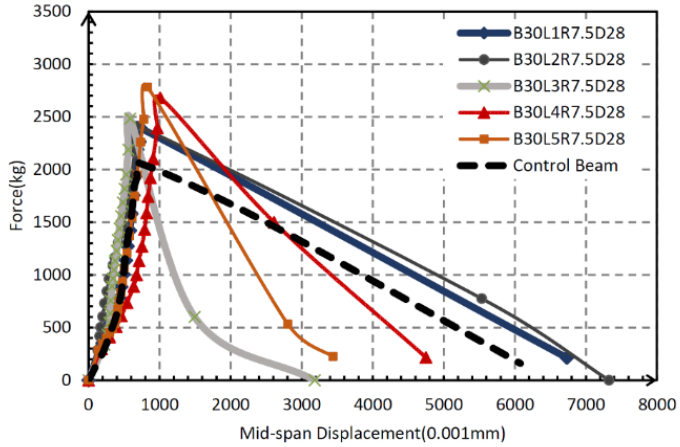

(b): B30 Specimens

Fig. 8. Load-displacement curves at the mid-span for the specimens with R=7.5.

4.1.2. Investigation of the peak load capacity for R=15 specimens

Table 4 presents the peak load capacity of the reinforced specimens with the ratio of R=15. Reinforcing the concrete beams with the ratio of R=15 indicated a significant effect on the peak load capacity compared to the reinforced specimens with the ratios of R=5 and R=7.5. In comparison with the Control Beams, the reinforcement of the concrete beams with 1 to 5 layers of the GFGM increased the peak load capacity from 22.1% to 48.6%, respectively.

Regarding the effect of layers in this R ratio, it was found that by increasing the number of GFGM layers to 5, $B_{25}L_5R_{15}D_{28}$ specimen indicated a significant effect on the peak load capacity. Furthermore, it was observed that the maximum peak load capacity was 21.76% and was related to the $B_{25}L_5R_{15}D_{28}$ specimen in comparison with the $B_{25}L_1R_{15}D_{28}$ specimen.

Table 3. Results of the peak load capacity for R=7.5 specimens.

specimens ID	B25		B30	
	Peak Load (Kg)	Relative Difference Compared to Control Beam (%)	Peak Load (Kg)	Relative Difference Compared to Control Beam (%)
Control Beam	1928.4	0.0	2062.9	0.0
$L_1R_{7.5}D_{28}$	2324.1	20.5	2391.4	15.9
$L_2R_{7.5}D_{28}$	2355.0	22.1	2412.8	17.0
$L_3R_{7.5}D_{28}$	2427.1	25.9	2483.4	20.4
$L_4R_{7.5}D_{28}$	2520.3	30.7	2678.9	29.9
$L_5R_{7.5}D_{28}$	2496.8	29.5	2783.5	34.9

Table 4. Results of the peak load capacity for R=15 specimens.

Specimen ID	B25		B30	
	Peak Load (Kg)	Relative Difference Compared to Control Beam (%)	Peak Load (Kg)	Relative Difference Compared to Control Beam (%)
Control Beam	1928.4	0.0	2062.9	0.0
$L_1R_{15}D_{28}$	2353.7	22.1	2428.7	17.7
$L_2R_{15}D_{28}$	2490.4	29.1	2680.5	29.9
$L_3R_{15}D_{28}$	2677.8	38.9	2713.3	31.5
$L_4R_{15}D_{28}$	2721.8	41.1	2993.5	45.1
$L_5R_{15}D_{28}$	2865.8	48.6	2889.6	40.1

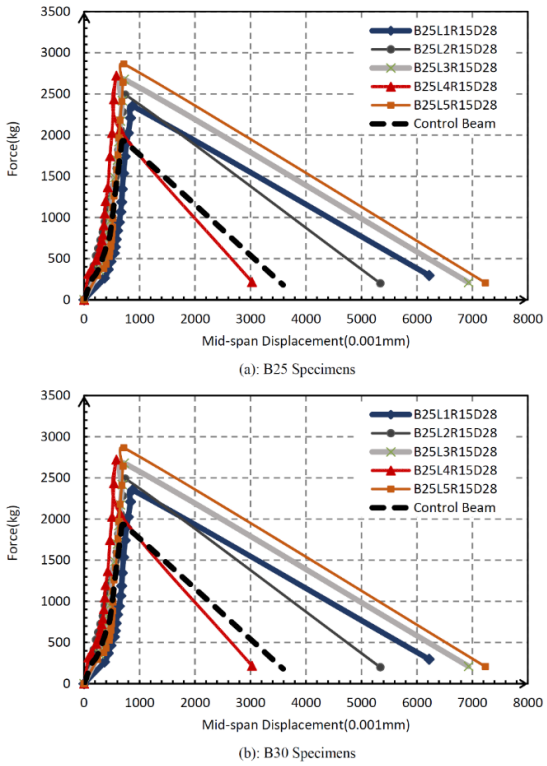

Fig. 9. Load-displacement curves at the mid-span for the specimens with R=15.

4.1. Investigation of the load-midspan displacement behavior

According to the (Fig. 7.- Fig. 9.) it was observed that for the specimens reinforced with R=5, R=7.5 and R=15, the maximum displacement at the mid-span corresponded to the concrete beams reinforced with two-layer, with the maximum number of layers, and with one-layer GFGM, respectively. All of the beams reinforced with R=5 indicated an approximately the same displacement. However, the beams reinforced with R=15 indicated an approximately the same displacement as the Control Beams at the mid-span. The displacement at the mid-span of the specimens reinforced with different R_k did not follow a specific pattern and indicated a post-track brittle behavior.

4.1. Investigation of the effect of different R ratios on the capacity of specimens

The selection of three ratios of R was due to the uncertainty of the complete bonding between the GFGM and the concrete. The specimens were firstly constructed with the ratio of R=5 and then were prepared with the ratio of R=15. The results and observations during the test indicated a complete bonding between the GFGM and the concrete. In the same regard, it was also observed

that the bonding between the GFGM and concrete was maintained for the specimens made with a 1 cm-concrete cover (R=15).

Table 5 and Fig. 10. show the peak load capacity of the concrete beams that have the same layer of number and different ratios of R. According to Table 5 and Fig. 10., it is observed that with increasing the ratio from R=5 to R=15, the peak load capacity increased as well. Furthermore, it was observed that the maximum increase of peak load capacity from R=5 to R=15 was related to the reinforced concrete beams with 4 layers of GFGM which was 26.70% and 32.14% for the B25 and B30 specimens, respectively. It should be noted that due to the complete bonding between the GFGM and concrete, the more the placement of the GFGM was close to the bottom of the concrete beam, the more peak load capacity increased.

Table 5. The recorded capacity of the specimens with different R ratios.

Specimen ID	B25			B30		
	R=5 Peak Load (Kg)	R=7.5 Peak Load (Kg)	R=15 Peak Load (Kg)	R=5 Peak Load (Kg)	R=7.5 Peak Load (Kg)	R=15 Peak Load (Kg)
L_1	2038.0	2324.1	2353.7	2106.7	2391.4	2428.7
L_2	2095.3	2355.0	2490.4	2155.7	2412.8	2680.5
L_3	2174.3	2427.1	2677.8	2256.4	2483.4	2713.3
L_4	2148.3	2520.3	2721.8	2265.4	2678.9	2993.5
L_5	2309.7	2496.8	2865.8	2335.8	2783.5	2889.6

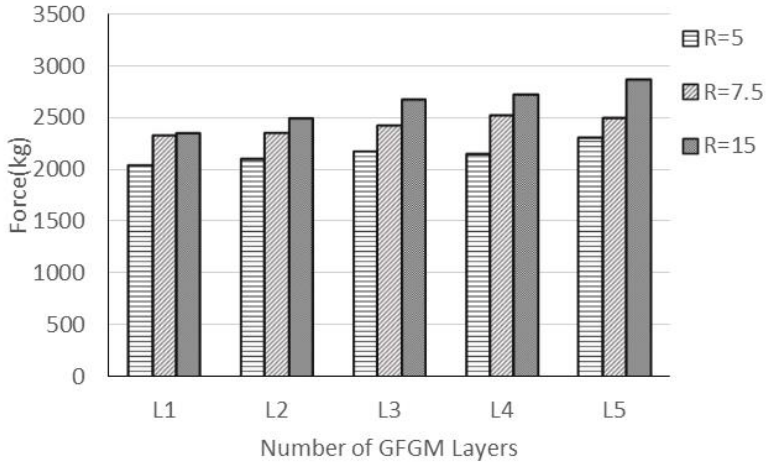

(a): B25 Specimens

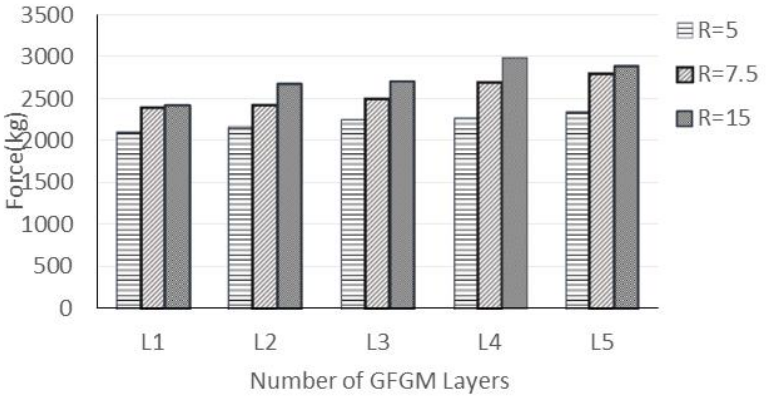

(b): B30 Specimens

Fig. 10. Comparison the recorded capacity of the specimens with different R ratios.

4.1. Investigation of the effect of curing time on the pick load capacity

All concrete beams were cured for 24 h in the molds covered with wet burlap at 23±1°C. After demolding the specimens, $B_iL_jR_kD_{28}$ and $B_iL_jR_kD_{90}$ specimens were cured in water at 23±1°C for 28 and 90 days, respectively, before being tested. Table 6 and Table 7, show the comparison between the peak load capacity of the 28-days and 90-days curing specimens. It was observed that increasing the curing time from 28 to 90 days increased the peak load capacity of the specimens to a significant amount. In this regard, the most peak load capacity increase was related to $B_{30}L_5R_5D_{90}$ specimen with 26.8% compared to $B_{30}L_5R_5D_{28}$ specimen. It should be noted that only the concrete beams constructed with R=5 and R=7.5 were left to cure for 28 and 90 days and the concrete beams constructed with R=15 were left to cure only for 28 days.

Table 6. Comparison of the effect of curing time on the capacity of specimens with R=5.

Specimens ID	B25			B30		
	D28 Peak Load (Kg)	D90 Peak Load (Kg)	% increase	D28 Peak Load (Kg)	D90 Peak Load (Kg)	% increase
L_1	2038.0	2406.9	18.1	2106.7	2470.9	17.3
L_2	2095.3	2413.8	15.2	2155.7	2530.9	17.4
L_3	2174.3	2423.3	11.4	2256.4	2643.4	17.2
L_4	2148.3	2693.9	25.4	2265.4	2862.6	26.4
L_5	2309.7	2777.8	20.3	2335.8	2961.9	26.8

Table 7. Comparison of the effect of curing time on the capacity of specimens with R=7.5.

Specimens ID	B25			B30		
	D28 Peak Load (Kg)	D90 Peak Load (Kg)	% increase	D28 Peak Load (Kg)	D90 Peak Load (Kg)	% increase
L_1	2324.1	2573.7	10.7	2391.4	2563.5	7.2
L_2	2355.0	2522.4	7.1	2412.8	2599.8	7.8
L_3	2427.1	2571.2	5.9	2483.4	2734.4	10.1
L_4	2520.3	2643.3	4.9	2678.9	2711.3	1.2
L_5	2496.8	2814.6	12.7	2783.5	3071.2	10.3

4. Conclusion

In the current study, the use of GFGM as the flexural reinforcement concrete beams was investigated. Fifty concrete beams reinforced with GFGM with different layers, placements, curing times and various concrete mixing designs (25 and 30 MPa) were constructed and tested under a three-point bending test. In this regard, six unreinforced beams with pure concrete were considered as Control Beams. The conclusions are as following:

Comparing the results of the GFGM reinforced concrete beams with the Control Beams showed an increase in peak load capacity of specimens so that the maximum increase was equal to 48.6%.

As the position of the GFGM is closer to the tensile face of the beam (R Changes from 5 to 15), the capacity of the beam has increased.

Regarding the concrete beams reinforced with the ratio of R=5, it was found that by changing the number of GFGM layers from 1 to 5, the peak load capacity increased from 5.68% to 19.77% compared to the Control Beam.

Regarding the concrete beams reinforced with the ratio of R = 7.5, it was found that by changing the number of GFGM layers from 1 to 5, the peak load capacity increased from 15.92% to 34.91% compared to the Control Beam.

Regarding the concrete beams reinforced with the ratio of R = 15, it was found that by changing the number of GFGM layers from 1 to 5, the peak load capacity increased from 17.73% to 48.61% compared to the Control Beam.

Changing the GFGM placement distance from the bottom face of the beam (from 3 cm to 1 cm) indicated significant effect on the bonding between the GFGM and concrete so that a complete bonding was observed in the nearest placement (1 cm which is correspond to R=15).

By increasing the curing time from 28 days to 90 days, the peak load capacity increased as well.

The displacement at the mid-span of the specimens reinforced with different R ratios did not follow a specific pattern.

Increasing the compressive strength of the concrete from 25 to 30 MPa did not have any significant effect on the flexural capacity of the GFGM reinforced specimens.

Funding

This research did not receive any specific grant from funding agencies in the public, commercial, or not-for-profit sectors.

Conflicts of interest

The authors declare that they have no known competing financial interests or personal relationships that could have appeared to influence the work reported in this paper.

Authors contribution statement

Mohammad Dashtpour: Data curation; Formal analysis; Investigation; Methodology; Resources; Software; Visualization; Roles/Writing – original draft.

Seyed Shaker Hashemi: Conceptualization; Investigation; Methodology; Project administration; Resources; Supervision; Validation; Writing – review & editing.

Mahmoud Malakouti Oloun Abadi: Resources; Software; Supervision; Validation; Visualization; Roles/Writing – original draft; Writing – review & editing.

References

[1] Janaki AM, Shafabakhsh G, Hassani A. Evaluation of Mechanical Properties and Durability of Concrete Pavement Containing Electric Arc Furnace Slag and Carbon Nanostructures. J Rehabil Civ Eng 2023;11,:1–20. https://doi.org/10.22075/JRCE.2021.23149.1499.

[2] Mehrinejad Khotbehsara M, Zadshir M, Miyandehi BM, Mohseni E, Rahmannia S, Fathi S. Rheological, mechanical and durability properties of self-compacting mortar containing nano-TiO2 and fly ash. J Am Sci 2014;10:222–228.

[3] Mehdizadeh B, Vessalas K, Ben B, Castel A, Deilami S, Asadi H. Advances in Characterization of Carbonation Behavior in Slag-Based Concrete Using Nanotomography. Nanotechnol. Constr. Circ. Econ. (NICOM 2022), Melbourne: 2023, p. 297–308. https://doi.org/10.1007/978-981-99-3330-3_30.

[4] Mehdizadeh Miyandehi B, Vessalas K, Castel A, Mortazavi M. Investigation of Carbonation Behaviour in High-Volume GGBFS Concrete for Rigid Road Pavements. 7th Concr. Pavements Conf., Wollongong: ASCP (Australian Society for Concrete Pavements); 2023.

[5] Parvin YA, Shaghaghi TM, Pourbaba M, Mirrezaei SS, Zandi Y. Flexural behavior of UHPC beams reinforced with macro-steel fibers and different ratios of steel and GFRP bars. J Rehabil Civ Eng 2024;12,:41–57. https://doi.org/DOI: 10.22075/JRCE.2023.28070.1695.

[6] Qian WM, Vahid MH, Sun YL, Heidari A, Barbaz-Isfahani R, Saber-Samandari S, et al. Investigation on the effect of functionalization of single-walled carbon nanotubes on the mechanical properties of epoxy glass composites: Experimental and molecular dynamics simulation. J Mater Res Technol 2021;12:1931–45. https://doi.org/10.1016/j.jmrt.2021.03.104.

[7] Arboleda D. Fabric Reinforced Cementitious Matrix (FRCM) Composites for Infrastructure Strengthening and Rehabilitation: Characterization Methods. Fac Univ Miami 2014.

[8] Rai A, Joshi YP. Applications and properties of fibre reinforced concrete. J Eng Res Appl 2014;4:123–31.

[9] Osgouei YB, Tafreshi ST, Pourbaba M. Flexural Properties of UHPFRC Beams with an Initial Notch. J Rehabil Civ Eng 2023;11:141–77. https://doi.org/10.22075/JRCE.2022.25513.1576.

[10] Simonsson E. Complex shapes with textile reinforced concrete-An investigation of structural form, material and manufacturing. Master of Science Thesis in the Master's Programme Structural Engineering and Building Technology, Chalmers University of Technology, Gothenburg, Sweden., 2017.

[11] Friese D, Scheurer M, Hahn L, Gries T, Cherif C. Textile reinforcement structures for concrete construction applications—a review. J Compos Mater 2022;56,:4041–64. https://doi.org/10.1177/00219983221127181.

[12] Rossi E, Randl N, Mészöly T, Harsányi P. Flexural strengthening with fiber-/textile-reinforced concrete. ACI Struct J 2021;118,:97. https://doi.org/10.14359/51732647.

[13] Nanni A. Concrete repair with externally bonded FRP reinforcement. Concr Int 1995;17,:22–6.

[14] Pirah JA, Mydin MAO, Nawi MNM, Omar R. Innovative Application of Interwoven Fiberglass Mesh to Strengthen Lightweight Foamed Concrete. J Adv Res Appl Sci Eng Technol 2022;28,:165–76. https://doi.org/10.37934/araset.28.3.165176.

[15] Jabr A. Flexural Strengthening of RC beams using Fiber Reinforced Cementitious Matrix. Phd Thesis, University of Windsor (Canada), 2017.

[16] Mat Serudin A, Othuman Mydin MA, Mohd Nawi MN, Deraman R, Sari MW, Abu Hashim MF. The Utilization of a Fiberglass Mesh–Reinforced Foamcrete Jacketing System to Enhance Mechanical Properties. Materials (Basel) 2022;15,:1–17. https://doi.org/10.3390/ma15175825.

[17] Ombres L. Concrete confinement with a cement based high strength composite material. Compos Struct 2014;109,:294–304. https://doi.org/10.1016/j.compstruct.2013.10.037.

[18] ACI-549.4R-13. Guide to design and construction of externally bonded fabric-reinforced cementitious matrix (FRCM) systems for repair and strengthening concrete and masonry structures. Am Concr Instutute 2013.

[19] Ramezani A, Esfahani MR, Sabzi J. Strengthening of reinforced concrete beams using fiber-reinforced cementitious matrix systems fabricated with custom-designed mortar and fabrics. Front Struct Civ Eng 2023;17,:1100–1116. https://doi.org/10.1007/s11709-023-0967-9.

[20] Faleschini F, Zanini MA, Hofer L, Toska K, De Domenico D, Pellegrino C. Confinement of reinforced concrete columns with glass fiber reinforced cementitious matrix jackets. Eng Struct 2020;218,:110847. https://doi.org/10.1016/j.engstruct.2020.110847.

[21] Chazallon C, Barazzutti C, Pelletier H, Nguyen ML, Hornych P, Mouhoubi S, et al. Reproduction of geogrid in situ damage used in asphalt concrete pavement with indentation tests. J Test Eval 2020;48,:60–71. https://doi.org/10.1520/JTE20180929.

[22] Lesueur D, Leguernevel G, Riot M. On the performance of geogrids for asphalt pavement reinforcement: laboratory evaluation and selected case studies. 7th E&E Congr 2021:1–11.

[23] Meng X, Chi Y, Jiang Q, Liu R, Wu K, Li S. Experimental investigation on the flexural behavior of pervious concrete beams reinforced with geogrids. Constr Build Mater 2019;215,:275–84. https://doi.org/10.1016/j.conbuildmat.2019.04.217.

[24] Tang X, Higgins I, Jlilati MN. Behavior of geogrid-reinforced Portland cement concrete under static flexural loading. Infrastructures 2018;3,:1–12. https://doi.org/10.3390/infrastructures3040041.

[25] Tang X, Chehab GR, Kim S. Laboratory study of geogrid reinforcement in Portland cement concrete. Proc 6th RILEM Int Conf Crack Pavements CRC Press Taylor Fr Group, London 2008:769–78. https://doi.org/10.1201/9780203882191.ch75.

[26] Al-Hedad ASA, Bambridge E, Hadi MNS. Influence of geogrid on the drying shrinkage performance of concrete pavements. Constr Build Mater 2017;146,:165–74. https://doi.org/10.1016/j.conbuildmat.2017.04.076.

[27] Erfan AM, Hassan HE, Hatab KM, El-Sayed TA. The flexural behavior of nano concrete and high strength concrete using GFRP. Constr Build Mater 2020;247,:118664. https://doi.org/10.1016/j.conbuildmat.2020.118664.

[28] Ahmed HQ, Jaf DK, Yaseen SA. Flexural strength and failure of geopolymer concrete beams reinforced with carbon fibre-reinforced polymer bars. Constr Build Mater 2020;231,:117185. https://doi.org/10.1016/j.conbuildmat.2019.117185.

[29] ASTM-C136/C136M. Standard Test Method for Sieve Analysis of Fine and Coarse Aggregates. ASTM Int WwwAstmOrg 2019.

[30] ASTM-C29 / C29M-17a. Standard Test Method for Bulk Density (“Unit Weight”) and Voids in Aggregate. ASTM Int WwwAstmOrg 2017.

[31] ASTM-C566-19. Standard Test Method for Total Evaporable Moisture Content of Aggregate by Drying. ASTM Int WwwAstmOrg 2019.

[32] ASTM-C127-15. Standard Test Method for Density , Relative Density (Specific Gravity), and Absorption of Coarse Aggregate. ASTM Int WwwAstmOrg 2013.

[33] ASTM-C-128. Standard Test Method for Relative Density (Specific Gravity) and Absorption of Fine Aggregate. ASTM Int WwwAstmOrg 2015.

[34] ASTM-C33/C33M - 18. Standard Specification for Concrete Aggregates. ASTM Int WwwAstmOrg 2018.

[35] ASTM-C188-17. Standard test method for density of hydraulic cement. ASTM Int WwwAstmOrg 2017.

[36] ASTM-C191-18. Standard Test Methods for Time of Setting of Hydraulic Cement by Vicat Needle. ASTM Int WwwAstmOrg 2018.

[37] ASTM-C109/109M-16a. Standard test method for compressive strength of hydraulic cement mortars (Using 2-in. or cube specimens). ASTM Int WwwAstmOrg 2016.

[38] ACI-211.1-91. Standard Practice for Selecting Proportions for Normal, Heavyweight, and Mass Concrete. Am Concr Institute Comm 1991.

[39] ASTM-C143/C143M. Standard Test Method for Slump of Hydraulic-Cement Concrete. ASTM Int WwwAstmOrg 2015.

[40] ASTM-C138/C138M − 17a. Standard Test Method for Density (Unit Weight), Yield, and Air Content (Gravimetric) of Concrete. ASTM Int WwwAstmOrg 2017.

[41] ASTM-C39/C39M-18. Standard Test Method for Compressive Strength of Cylindrical Concrete Specimens. ASTM Int WwwAstmOrg 2018.

[42] ACI-308. Guide to Curing Concrete. Am Concr InstituteInstitute 2001.

[43] ASTM-C293. Flexural Strength of Concrete (Using Simple Beam With Center-Point Loading). ASTM Int WwwAstmOrg 2016.